DOI:
10.1021/acs.macromol.8b02509

Document Version
Peer reviewed version

Pseudo-Polyrotaxanes of Cyclodextrins with Direct and Reverse X-shaped Block-Copolymers: a Kinetic and Structural Study

Joan Puig-Rigall[1], Rafael Serra-Gómez[1], Ian Stead[2], Isabelle Grillo[3], Cécile A. Dreiss*[,2] and Gustavo González-Gaitano*[,1]

[1] Departamento de Química, Universidad de Navarra, 31080 Pamplona, Spain
[2] Institute of Pharmaceutical Science, King's College London, Franklin-Wilkins Building, 150 Stamford Street, London SE1 9NH, UK; cecile.dreiss@kcl.ac.uk
[3] Institut Laue-Langevin, 71 avenue des Martyrs, B.P. 156, 38042 Grenoble Cedex, France; grillo@ill.fr
***** Correspondence: gaitano@unav.es

Abstract

Pseudo-polyrotaxanes (PPRs) are supramolecular host-guest complexes constituted by the reversible threading of a macrocycle along a polymer chain, which offers potential applications in nanotechnology, drug delivery and biomaterials. We report the threading of cyclodextrins (CDs), cyclic oligosaccharides, onto X-shaped PEO-PPO block-copolymers, with two opposite presentation of their hydrophobic and hydrophilic blocks: Tetronic 904 (T904), and its reverse counterpart, Tetronic T90R4. We assess the effect of relative block position on the polymeric surfactants and cavity size of CD have on the composition, morphology, thermodynamics and kinetics of PPRs by using a combination of X-ray diffraction, Scanning Electron Microscopy (SEM), NMR, UV-Vis spectroscopy and Time-Resolved Small-Angle Neutron Scattering (TR-SANS). Solid PPRs with lamellar microstructure and crystalline channel-like structures are obtained with native CDs and both Tetronics above a threshold concentration of the macrocycle, which varies with the type of CD and surfactant. While γ-CD can form PPRs with both Tetronics, α-CD only form a PPR with T90R4 at high concentrations. The results can be explained in terms of

the preferential complexation of α-CD with EO and γ-CD with PO monomers, which also has a direct impact on the kinetics of PPR formation. Thermodynamic parameters of the reaction were obtained from the analysis of the stoichiometries and threading times as a function of temperature by using a model based on the Eyring equation. Negative enthalpies and positive entropies are obtained in all cases, and reactions are thermodynamically most favorable in the case of α-CD with T904 and γ-CD with T90R4. TR-SANS experiments reveal an increase in the radius of gyration of the unimers over time, consistent with CD threading and expansion of the PPR. Above the CMT, α-CD threads the unimers to form the PPR, with no effect on the structure of T904 micelles, whose volume fraction decreases due to the shift of micellization equilibrium.

Keywords: cyclodextrins; host-guest; Tetronic; block copolymers; polyrotaxanes; small angle neutron scattering; kinetics of threading

1. Introduction

Polyrotaxanes (PRs) are supramolecular mechanically interlocked structures in which a polymer, acting as a polytopic guest, threads a number of macrocycles (host) to form a "molecular necklace".[1] In a PR, the threaded rings, bound by non-covalent interactions, are confined to the polymeric chain by bulky terminal stoppers, allowing some sliding along the macromolecule but preventing its dethreading. In the absence of terminal stoppers, the resulting structure is called a pseudo-polyrotaxane (PPR): macrocycles are free to enter and escape the polymeric chain, according to the laws of chemical equilibrium and kinetics.[2,3] The 2016 Nobel Prize in Chemistry, granted to Sir J. Fraser Stoddart for his work on "the design and synthesis of molecular machines",[4] mainly deals with the threading of

macrocycles on an axle, which can then be "used for new materials, sensors, and energy storage systems".[5,6] Thus, PRs and PPRs constitute the starting point of interesting supramolecular structures and are attractive building blocks for applications in the biomedical field[7–10] and other technological fields, such as elastic binders for silicon microparticle anodes in lithium ion batteries,[11] solid polymer electrolytes (SPEs),[12] or hybrid and thermoresponsive aerogels,[13,14] to mention just a few.

Most of the PRs and PPRs reported in the literature are produced with cyclodextrins (CDs), which are cyclic oligosaccharides formed by the association of several glucopyranose units in a toroid like arrangement.[15] The size of the cavity, which depends on the number of glucopyranoses (α-, β-, and γ-CDs, containing respectively 6, 7, and 8 glucose units) determines the affinity for a specific polymer,[16] while the capacity to form hydrogen-bonds between adjacent CDs contributes to stabilize the resulting supramolecular structure, with a preferred orientation in a head-to-head and a tail-to-tail arrangements, given the toroidal shape of the CDs.[17,18] Less regular configurations of threaded CDs, which lead to soluble PPRs, have also been reported recently.[19] The synthesis, characterization and mechanism of threading of PRs and PPRs based on CDs and different polymers, have been extensively reviewed in the literature,[2,3,20] as well as their potential applications in biomedicine, particularly in drug delivery, or biomaterials, such as hydrogels and scaffolds in tissue engineering.[9,10,21–23]

The first PPR based on CDs was reported by Harada in 1990,[24] and obtained from the complexation of PEG and α-CD in water, with a composition of 2 ethylene oxide (EO) units per CD. Harada also established that the binding is very selective, depending on the type of CD and monomer:[1,24,25] α-CD only forms stable inclusion complexes with PEG, while the threading does not occur with polypropylene glycol (PPG); instead, β- and γ-CD form PPRs with PPG but not with PEG.[17,18,24] This geometrical selectivity based on the

cavity size of CDs opens up interesting prospects with block copolymers, where only one of the two blocks can be accommodated by a given macrocycle.[26] A family of classic block-copolymers that has been widely studied is poloxamers, better known by their commercial name of Pluronics® (BASF). Pluronics are linear polymeric surfactants with a PEO-PPO-PEO block structure. The number of PO and EO monomers that form the arms can be varied, offering a wide range of molecular weight and hydrophobic-lipophilic balance (HLB) values. By controlling their concentration and temperature, Pluronics self-assemble into micelles and gels in aqueous media.[27–31] The interaction between native CDs and Pluronics leading to the formation of PRs and PPRs has been described in the literature.[32,33] The substitution of the hydroxyl groups on the rims of the CD strongly modifies the aggregation behavior of the Pluronic micelles, depending on the specific nature of the substituents,[34–36] and the kinetics and mechanisms of the formation of the PPRs have been studied.[37–39] Specifically, the PRs formed with 2-hydroxypropyl β-CD and Pluronic have shown promise in the biomedical field for the treatment of Niemann-Pick disease.[40–42]

Another type of block-copolymers of interest as guests for cyclodextrins is poloxamines, also known by their commercial name of Tetronic® (BASF). They present a 4-arm star shape, where each of the arms is made of PEO and PPO blocks connected by a central ethylene diamine spacer. Their pH-responsiveness due to the protonation of the central diamine group at acidic pH and their capacity to inhibit ATP-binding cassette transporters in cancer cell lines, responsible for multidrug resistance,[43,44] in addition to other characteristics they share with Pluronics, like self-assembly and amphiphilic character, make Tetronics a promising copolymer to be used in the formation of PPRs. There are very few studies on PPRs based on poloxamines, mostly by us [45–48] and some other groups.[49,50] In particular, the kinetics of PPRs formation with native CDs and the effect of temperature and aggregation state have not yet been studied.

Within this framework, we have investigated in this work the effect of: the type of cyclodextrin, the relative distribution of PEO and PPO blocks of the poloxamines, and temperature, on the structure of PPRs and the thermodynamics and kinetics of formation. We have focused on the most soluble native CDs, α- and γ-CD, and two Tetronic surfactants, T904 and T90R4, which present a very similar PEO and PPO block length and composition but are the reverse structure from each other. While T904 has its PEO blocks as the external blocks, which makes it fairly hydrophilic and capable of forming micelles, T90R4 has its PPO blocks on the outside and does not micellize. The structure and morphology of the PPRs have been determined by X-ray diffraction and scanning electron microscopy (SEM), while their formation and composition have been studied by gravimetric analysis and NMR spectroscopy. A detailed kinetic analysis has been performed to study the effect of temperature, type of CD and Tetronic on the formation and subsequent aggregation of the PPRs, by using Time-Resolved SANS (TR-SANS) and UV-Vis spectroscopy, respectively.

2. Materials and Methods

Materials. Native cyclodextrins: α-cyclodextrin (≥98%) and γ-cyclodextrin (≥98%) (water contents of 10% for both CDs, as determined by TGA) were obtained from Sigma-Aldrich. Reverse Tetronic® 904 (T90R4) was purchased from Sigma-Aldrich, and Tetronic® 904 (T904) was a gift from BASF (Ludwigshafen, Germany). The reported composition per arm is 15 EO and 17 PO (T904, average molecular weight 6,700 $gmol^{-1}$) and 16 EO and 18 PO (T90R4, average molecular weight 7,200). PEG1000 was obtained from Fluka (Germany). All the solutions were prepared by weight, unless stated otherwise, and the concentrations are expressed in wt%.

Gravimetric analysis and determination of PPR composition. Weighed solutions of 1% T904 and 1% T90R4 in de-ionised water were added to varying amounts of CDs. The

samples were then vortexed for 1 minute and placed in an ultrasonic bath (FB11203, Fisherbrand, UK) for 10 minutes at 37 kHz and 80% power. The samples were left to react for 24 hours. After that time, the Eppendorfs were centrifuged for 10 minutes at 13000 rpm, the supernatant removed and the precipitates left to dry for 24 hours in a drying cabinet. The yield was obtained from the difference of mass with the empty Eppendorf as the mass of solid divided by the total mass of reactants. Standard deviation estimates of 2.8 and 1.2 are obtained for low (< 25%) and high (> 25%) yields, respectively, after duplicate experiments at 2% and 12% concentrations of γ-CD.

NMR spectroscopy. Samples were prepared by re-dissolving a small amount of the dried precipitate in 500μL of DMSO-d6 (deuterium content > 99%) to fully dissociate the complex. After 24 h, 1D 1H-NMR spectra were recorded with a Bruker Advance 400 MHz spectrometer. The number of CDs per Tetronic arm is calculated by measuring the areas of selected resonances from the polymer and the macrocycle in accordance with the following equation:

$$CDs/arm = \frac{A_{H1}/n}{A_{CH_3}/(3N_{PO})} \quad (1)$$

where A_{H1} and A_{CH3} are the areas of the signals from the outer H1 hydrogens of the CD and the methyl protons of the PO monomer of the Tetronic, respectively; n is the number of glucose units in the macrocycle (6 for α- and 8 for γ-CD); and N_{PO} the number of PO monomers per arm (17 for T904 and 18 for T90R4 in each PPO block).

Kinetic analysis by UV-vis spectroscopy. UV-visible spectra were recorded on an Agilent 8453 diode array spectrophotometer (2 nm resolution). Samples were placed in 1 cm path-length quartz cuvettes with magnetic stirring and temperature control incorporated (± 0.1 ºC, Quantum Northwest TC 1 accessory). The conditions set were 400 nm wavelength, a stirring speed of 1200 rpm, and variable time intervals to sample over the reaction to

produce a kinetic curve. The concentrations of CDs, T904 and T90R4 were adjusted in order to be in a regime where a PPR precipitate is eventually produced, based on the gravimetric experiments. Maximum working temperatures of 74 and 37 ºC were used in the cell for T904 and T90R4, respectively, below their cloud point (LCST).

X-ray diffraction (XRD). Solid PPRs were analyzed at room temperature by wide angle X-ray powder diffraction (XRD) in a Bruker D8 Advance diffractometer using the Cu Kα1 radiation from 2˚ to 80˚ (2θ), each 0.02˚ and 3 s per step. Solid samples were produced by sonication (Branson 2800 ultrasonic bath) according to the gravimetric and UV-vis data obtained previously. Once the reaction was complete, the mixtures were centrifuged at 20 ºC, during 30 minutes at 8000 rpm. The precipitate was then washed with 15 mL of water to remove the excess of CD. After centrifugation, the precipitate was frozen at -80 ºC for at least two hours and freeze-dried in a Telstar Cryodos lyophilizer.

Time-Resolved SANS (TR-SANS). Kinetic SANS experiments were carried out on the D22 diffractometer at the Institut Laue-Langevin (ILL), incorporating a stopped-flow unit (Biologic SFM-300), which allows for rapid mixing of several solutions and triggers the reaction with data acquisition. Neutrons wavelength was 6 Å, sample-to-detector distance 4 m, with a collimation at 5.6 m and a detector offset of 400 mm, giving a wave vector range $1.2 \times 10^{-2} < q < 0.26$ Å^{-1}, with a 7×10 mm^2 sample aperture. The cell path length used was 1 mm and the temperature was set to either 25ºC or 40ºC. The stock solutions of Tetronic and CD were prepared by weighing the required amounts of each compound and deuterated water. Appropriate volumes of stock solutions (total of 250 µL) were then mixed in the stopped-flow cell at a flow rate of 3 mL/s to obtain the target concentrations. Datasets of the experiments can be found on the ILL website.[51] SANS curves fitting was performed with SasView 4.2.0 software[52] in batch mode (data handling and fitting procedure and models used are described in Results and Discussion, SI and ref [53]).

Scanning Electron Microscopy (SEM). Surface morphology of the PPRs was examined with a desktop SEM (Phenom Pro microscope). Samples measured were those used for XRD experiments but with an extra recrystallization of the precipitate with water instead of freeze-drying. Prior to examination, samples were gold sputter-coated, with an 8 nm coating to render them electrically conductive. Images were acquired after 27 s of exposure time with resolution ≤ 10 nm.

3. Results and Discussion

3.1. Evidence of pseudo-polyrotaxane formation

When mixing solutions of native CDs and Tetronics, a PPR forms by threading of the host through the polymeric chain of the polymer. The CDs threaded on adjacent sites interact through hydrogen bonding, leading to the bundling of the PPR chains and eventually a phase separation, as hydrogen bonds between the polymer and water are hindered. This process is detected visually first by the onset of haziness in the solution, followed by the precipitation of the aggregated PPRs. Depending on the type of CD, the macrocycle interacts preferentially with the hydrophilic (PEO) or hydrophobic (PPO) blocks of the macromolecule. We have worked in this investigation with α- and γ-CD which, due to their higher solubility in water compared to β-CD (145, 19 and 232 $g \cdot L^{-1}$ for α, β and γ-CD, respectively),[15] produce superior yields for the complex.

The formation of a crystalline inclusion complex is typically verified by XRD. Focusing on α-CD (which displays a faster complexation reaction compared to γ-CD), the diffractograms show neat diffraction peaks that differ from those of the crystalline α-CD, with major peaks at 2θ = 5.0˚, 13.4˚, 14.4˚, 18.9˚ and 20.4˚ (Figure 1). The diffractogram obtained for a mixture of T904 with α-CD shows reflections at 2θ = 7.5˚, 13˚, 19.9˚, 22.7˚, very similar to those obtained from the mixtures of α-CD with PEG (Figure 1), obtained

under the same conditions, reflecting a similar type of packing. The mixture of α-CD with the reverse Tetronic, T90R4, generates similar diffraction peaks, but some of them are slightly shifted to lower angles compared to the direct poloxamines (for instance, the intense peak at $2\theta = 19.9^\circ$ is shifted to 19.6°). In both cases, the presence of a strong diffraction peak at approximately 20° is the signature of a PPR,[54,55] and reflects the channel-like structure caused by the packing of CDs threaded onto the polymeric chain, which are stabilized by hydrogen bonding.

SEM images of the precipitates obtained from mixtures of α-CD and T904 reveal a porous microstructure, organized in lamellae, reminiscent of the appearance of gypsum "desert rose" crystals, with an average thickness of the lamellae of 188 ± 36 nm (Figure 2). These structures are similar to those reported in the literature for linear[56] and four-branched star-poly(ε-caprolactone) PPRs with CDs.[57]

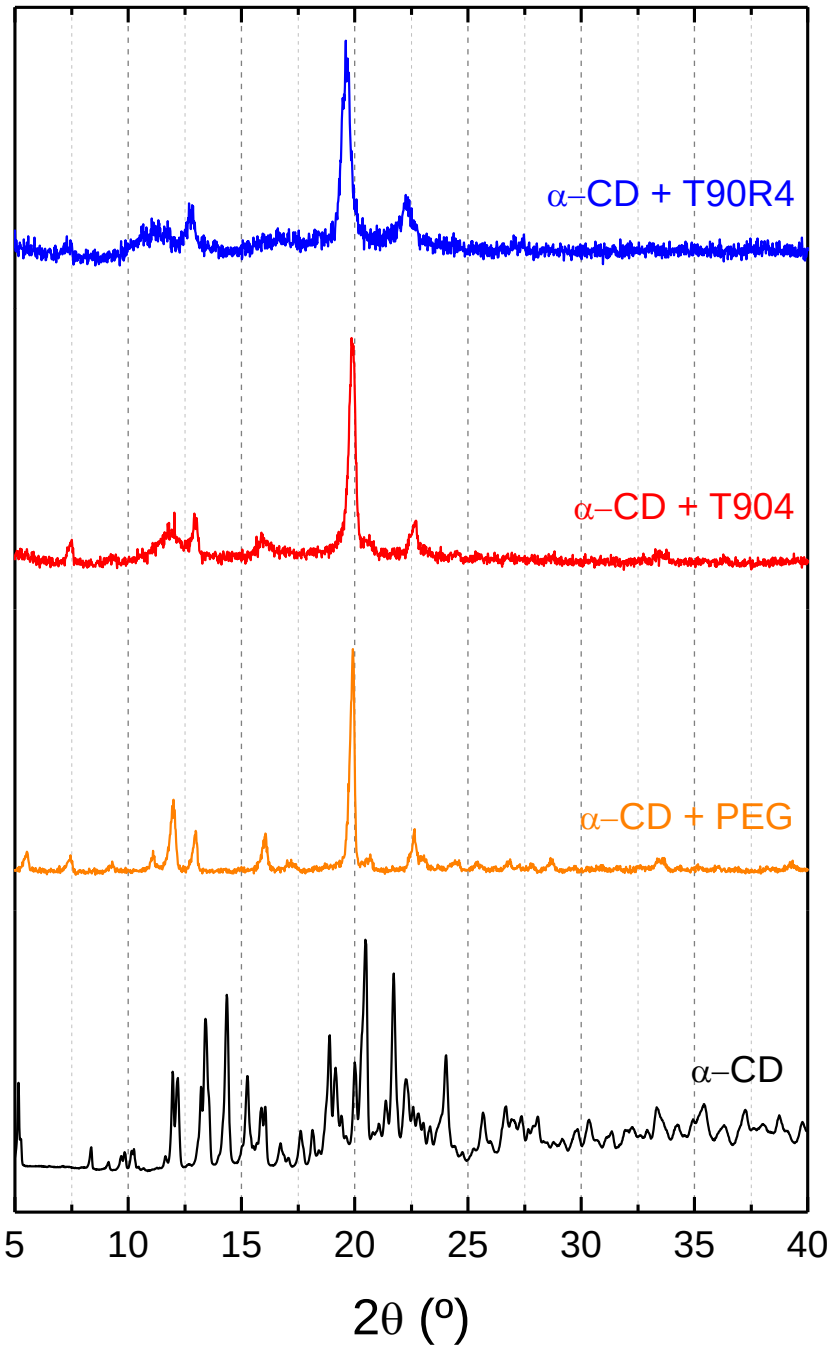

Figure 1. Wide angle XRD diffractograms of α-CD alone and the PPRs formed in mixtures of 5% α-CD with 0.66% PEG1000; 5% α-CD with 1% T904; 10% α-CD with 1% T90R4 (polymer concentrations adjusted to obtain the same molar ratio of EO).

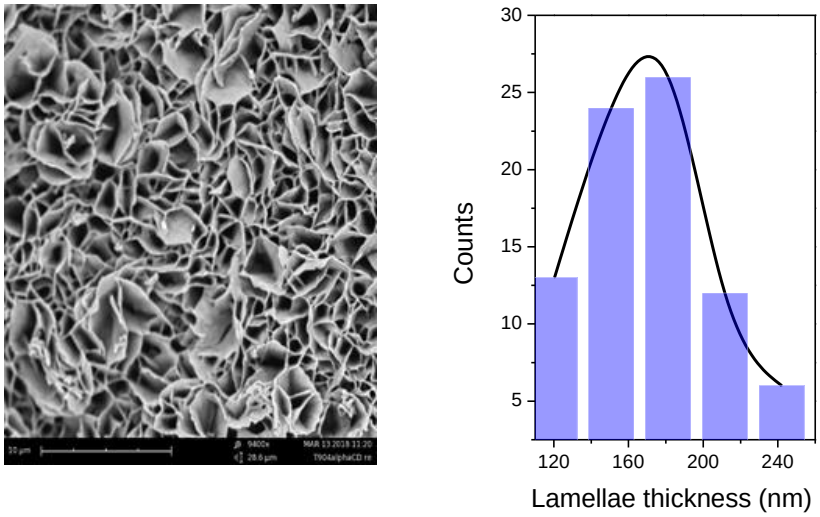

Figure 2. SEM micrograph of the precipitate obtained from the reaction of 5% α-CD with 1% T904 and thickness distribution of the lamellae.

3.2. Yield and stoichiometry of pseudo-polyrotaxanes

The chemical equilibrium that is established between CD and Tetronic requires a high enough number of CDs to thread before subsequent aggregation and precipitation of the PPRs occurs.[8] The reaction yield of the reaction was obtained by gravimetric analysis, calculated as mass precipitate divided by the total mass of reactants (Figure 3). In mixtures of T904 with α-CD, the precipitate is obtained above 4% CD, while with the reverse Tetronic, T90R4, the precipitate only appears above 8% CD, and gives lower yields (Figure 3A). In contrast, with the larger macrocycle, γ-CD, the precipitate is formed with both Tetronics over the whole range of concentrations studied, although higher yields are obtained for the reverse T90R4 (Figure 3B). These results can be rationalized from the preferential complexation of α-CD with EO monomers,[32] and γ-CD with PO ones.[33] In the direct Tetronic structure (T904), the terminal PEO blocks are easily accessible to the α-CD, whereas in the reverse configuration (T90R4), the macrocycles must thread over the PPO blocks to preferentially localize on the PEO,[58] which may explain the lower PPR yields and the higher concentrations of α-CD needed to achieve complexation. In fact, the shift of the

characteristic XRD reflections of the PPR with T90R4 to lower angles (Figure 1), would indicate a slightly higher separation distance between planes, consistent with the distortion of the cyclic structure of the CD to some extent. In the case of γ-CD, which has a wider cavity, the formation of PPRs with both T904 and T90R4 over the whole range of concentrations (Figure 3B) may be explained by the easier accessibility of PPO blocks, either because they are on the outside (T90R4) or because PEO blocks are not bulky enough to impede the threading of this large macrocycle, allowing its interaction with the inner hydrophobic PPO blocks (T904). The slightly higher yields obtained with the reverse poloxamine may be explained by the partial threading of the central PEO block, in which some γ-CDs would be 'sandwiched' between the fully covered PPO blocks.

The composition of the PPRs, in terms of the number of threaded CDs per chain, can be determined by signal integration in 1D NMR spectra, as explained in Materials and Methods. As a general trend, the number of threaded CDs increases with the concentration of the macrocycle (Figure 3), and at the highest concentration of CD studied (12%) the number of macrocycles per arm is nearly the same, around 10, for both α- and γ-CD. However, while in the case of α-CD this number seems to level off (Figure 3C), with γ-CD the number of CDs per arm is still increasing at 12% (Figure 3D).

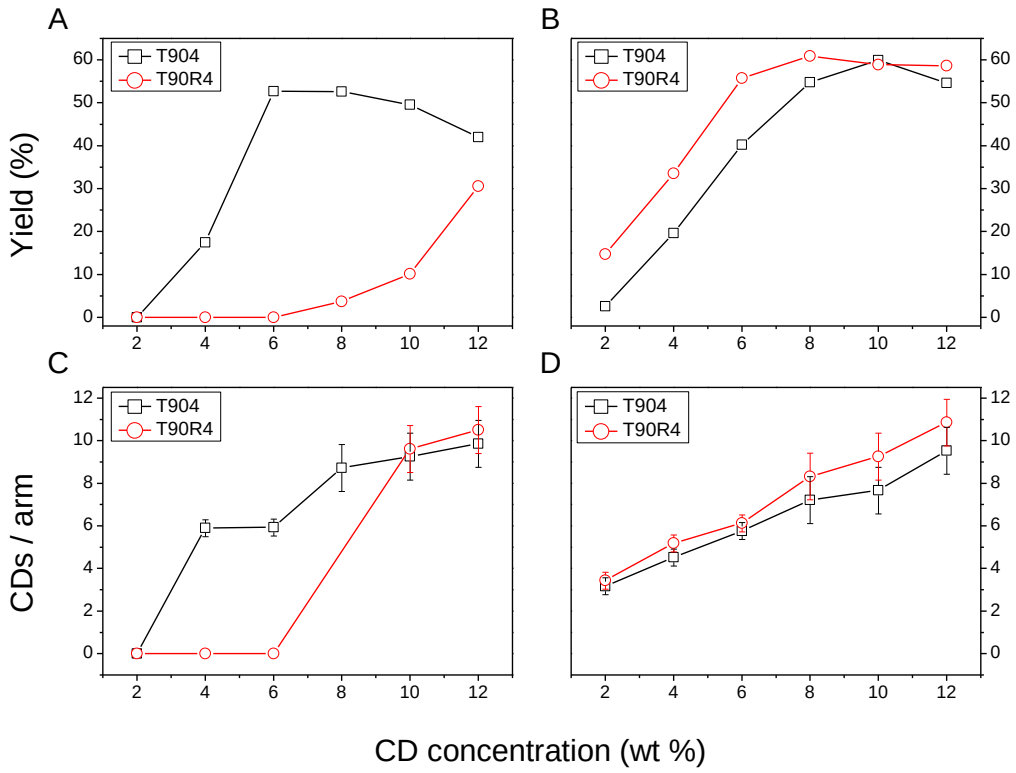

Figure 3. A and B: Yields obtained for the CD-Tetronic PPR formation after 24 hours; C and D: Number of cyclodextrins per arm of poloxamine. In both cases, 1% T904 or T90R4 was used with α-CD (A and C) and γ-CD (B and D).

From these results, the percentage of Tetronic and CD that react can be quantified (SI, Figure 1). It is worth mentioning that a certain amount of Tetronic and CD, at least 10 and 40 % (in moles), respectively, do not take part in the insoluble PPR, in other words, the supernatant contains the soluble PPR along with unreacted CD and poloxamine.

3.3. Kinetics of PPRs formation

The self-aggregation of the PPRs produces insoluble crystalline complexes which makes turbidimetry (the loss of intensity of transmitted light due to scattering) a suitable method to monitor the reaction of complexation.[59–61] Figure 4 shows the kinetic profile for 5% α- or γ-CD with 1% Tetronic, characterized by a sigmoidal curve, in which different regions can be distinguished, according to Lo Nostro et al.[60] The first region, in which the

absorbance is nearly zero, corresponds to the threading and sliding of the CDs onto the polymeric chain, characterized by a threading time, t_{th}, or lapse required to record a detectable increment in the absorbance.[60,62] Beyond this point, aggregation of the fully formed PPRs takes place and, as a result, the scattering increases quickly until the turbidity levels off.

The cavity size and the relative position of the blocks impact the kinetics of the PPR formation (Figure 4). For example, with α-CD, important differences can be observed between T904 and T90R4. While the precipitate is rapidly formed with T904, no increase in absorbance occurs with T90R4, reflecting the lack of solid PPR formation under these conditions, as already established (Figure 3A). The cavity of this CD is small and thus can enter through the PEO block (T904) but not the PPO ones (T90R4). In contrast, with the larger γ-CD, similar kinetic curves are obtained for both Tetronics, in line with the results shown in Figures 3B and 3D. Despite the reduced affinity of γ-CD for EO, which makes the reaction slower, and as a difference to α-CD, this wider CD can slide through the whole arm, leading to a solid PPR once enough CDs have been incorporated to the polymer.

At 5% CD and 1% polymer the reaction is relatively slow and it is possible to determine the evolution of the precipitate composition by NMR as a function of time by sampling at different time points. The results are plotted in SI, Figure 2. Interestingly, the number of threaded γ-CDs remains constant, with 5 and 6.5 CDs per arm of Tetronic for T90R4 and T904, respectively, confirming that, once the polymeric chain has incorporated a critical number of CDs, it precipitates as a solid PPR.

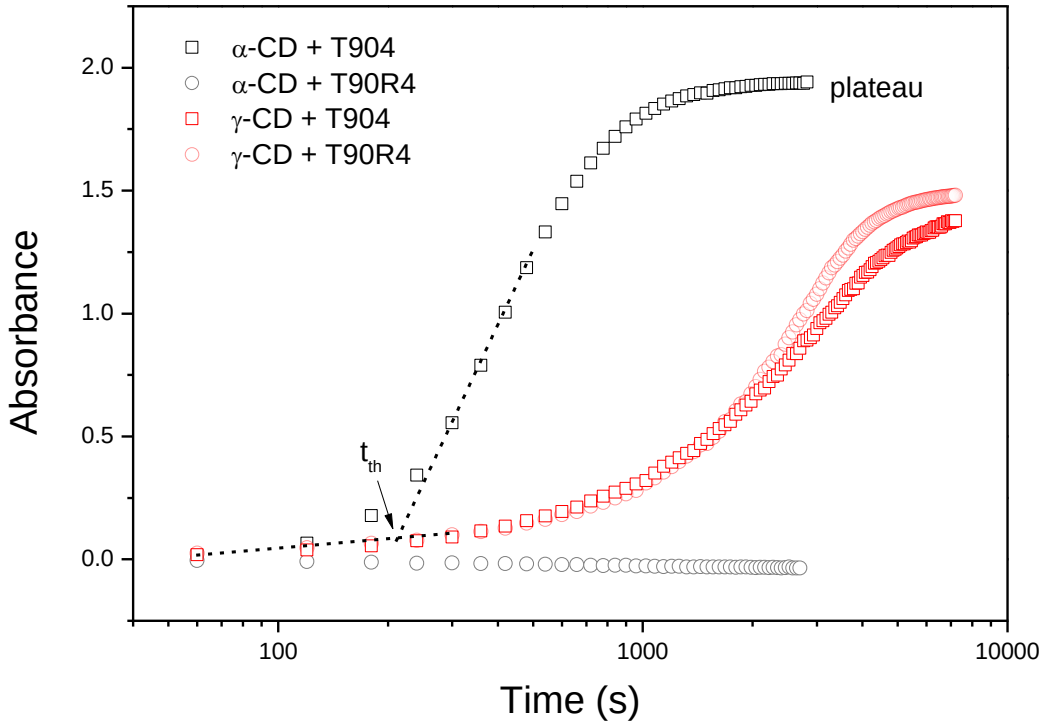

Figure 4. UV-Vis kinetic profile of 5% of CD (α- or γ-CD) with 1% Tetronic (T904 or T90R4) at room temperature. The solid lines correspond to the fit of a logistic function to the kinetic data.

3.4. Effect of temperature and thermodynamics of PPRs formation

The rate of threading of cyclodextrins on polymer chains is known to be temperature-dependent.[60,62] Increasing the temperature should favor the diffusion of both reactants and dethreading, while low temperatures usually promote the initial threading of the CDs through the polymer ends and the further sliding of the macrocycles, given the exothermic character of the CD complex formation. While the impact of the kinetics of complexation has been studied with linear polymers, PEG in particular,[60,62] there are very few studies on the kinetics of threading on polymers with more complex architectures,[60] such as the poloxamines studied here. In this work, several parameters need to be considered: (i) the macrocycles have a preferential affinity for either one or the other block (α-CD for the PEO and γ-CD for the PPO); (ii) the direct Tetronic, T904, self-assembles into micelles above the CMC (1%

wt at 35ºC);[48] (iii) the reverse Tetronic, T90R4 presents a LCST at a relatively low temperature (37 ºC). Due to this complexity, the reaction with T90R4 is studied between 10 and 35 ºC, while the complexation with T904 is considered over two distinct regions, covering unimers (10-30ºC) and micelles (35-50 ºC).

The corresponding kinetics were carried out over these temperature ranges with α-CD and γ-CD with both poloxamines, following the procedure described above. The threading times (t_{th}) obtained are presented in Figure 5.

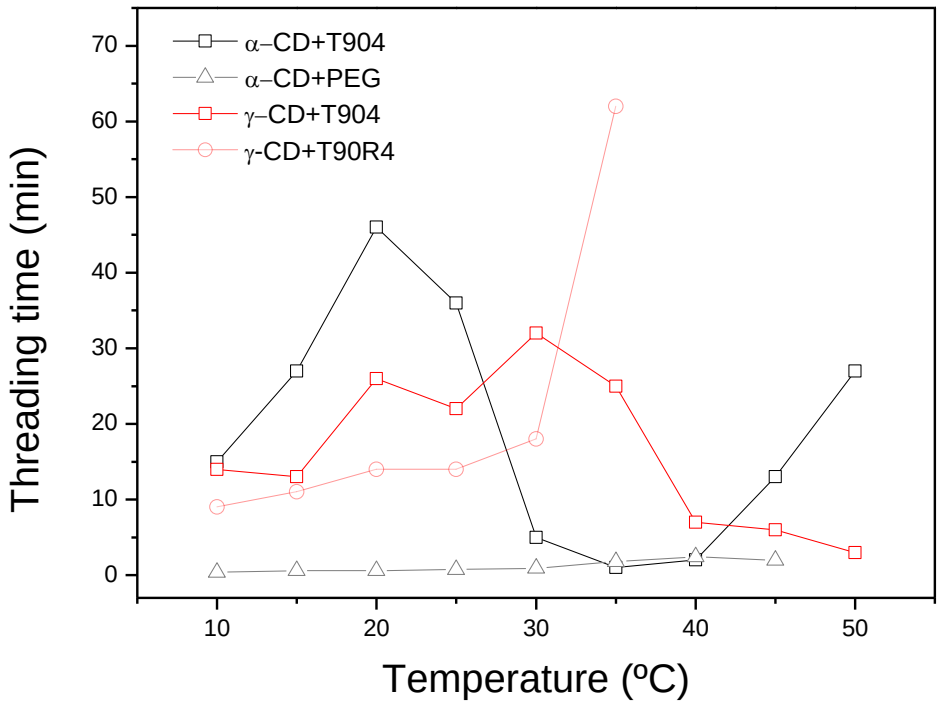

Figure 5. Threading times (t_{th}) obtained from turbidimetry for the reaction of 0.66% PEG1000 and 1% T904 and T90R4 with 5% α- and γ-CD.

The thermodynamics of threading were studied using the theoretical framework described by Ceccato et al. [62] and Becheri et al. [63] for CD-based PPRs. Briefly, by applying the activated-complex theory and according to Eyring theory, where the PPR is produced as soon as the activated state is formed, the equation that connects the thermodynamic parameters with the threading time is:

$$ln\frac{1}{Tt_{th}} = ln\frac{3k_B}{2h} + m\ln[CD] + \frac{\Delta S^{\neq}}{R} - \frac{\Delta H^{\neq}}{RT} \quad (2)$$

where T is the absolute temperature; t_{th} the threading time; m the number of CDs threaded per Tetronic molecule; [CD] is the molar concentration of cyclodextrins; k_B, h and R are the Boltzmann, Planck and universal gas constants, respectively; and $\Delta H^{\neq}$, $\Delta S^{\neq}$ the enthalpy and entropy of activation for the threading reaction. Given the relatively narrow range of temperatures studied, it is safe to assume that $\Delta H^{\neq}$ and $\Delta S^{\neq}$ are constant, as well as m (extracted from the experiments shown in Figure 3). The thermodynamic parameters can be obtained from the slope and intercept of the line obtained by plotting $-ln(Tt_{th})$ against the reciprocal of the temperature (Eq. 2). From $\Delta S^{\neq}$ and $\Delta H^{\neq}$ values, $\Delta G^{\neq}$ is readily obtained ($\Delta G^{\neq} = \Delta H^{\neq} - T\Delta S^{\neq}$). The results obtained within this theoretical framework are shown in Table 1 and are discussed for each of the three reactions considered.

Table 1. Thermodynamic parameters of PPR formation obtained from mixtures of either α- or γ-CD (5%) with 1% T904, 1% T90R4 or 0.66% PEG1000

	***T* range (ºC)**	**CDs / arm***	**$\Delta H^{\neq}$**	**$\Delta S^{\neq}$**	**$\Delta G^{\neq}$**
γ-CD + T90R4	10 - 30	5.5	-26 ± 3	203 ± 12	-86 ± 6
γ-CD + T904	10 - 30	5	-35 ± 10	116 ± 46	-69 ± 24
α-CD + T904	10 - 20	6	-79 ± 2	10 ± 11	-81 ± 5
α-CD + PEG	10 - 45	5**	-42 ± 5	71 ± 22	-63 ± 12

Enthalpies and Gibbs energies are expressed in kJ·mol^{-1} and entropies in J·mol^{-1}K^{-1}. (*) Number of CDs per arm are obtained from NMR (Figure 3), where m = 4 × CDs/arm. (**) From Ceccato et al.[62]

Pseudo-polyrotaxane formation of γ-CD with T90R4 and T904

T90R4 has the PPO blocks on the exterior; since γ-CD mainly interacts with the PO groups, the threading of this macrocycle is kinetically favored. The kinetic profiles are shown in Figure 6A from 10 to 35 ºC. A small and linear decrease of the reaction rate with temperature is observed between 10 and 30 ºC, while at 35 ºC, t_{th} is four times higher than at 30 ºC (Figure 5), most likely due to the proximity of the cloud point, where the disappearance of T90R4 unimers is not only associated with complexation, but also with a phase transition. Plotting the data according to Eq. 2 gives a linear plot, which was used to study the thermodynamics of the reaction (Figure 6B, Table 1). $\Delta H^{\neq}$ and $\Delta S^{\neq}$ values show that the overall process is exothermic, i.e., low temperatures promote the threading, and the entropy increases, resulting in a negative $\Delta G^{\neq}$ that reflects a spontaneous process over the temperature range studied, and practically independent on *T*. Given the affinity of γ-CD for PPO and considering that each γ-CD can lodge two POs, 11 PO groups would be complexed and 7 would remain exposed. Therefore, it seems unlikely that this CD can be threaded on the PEO blocks.

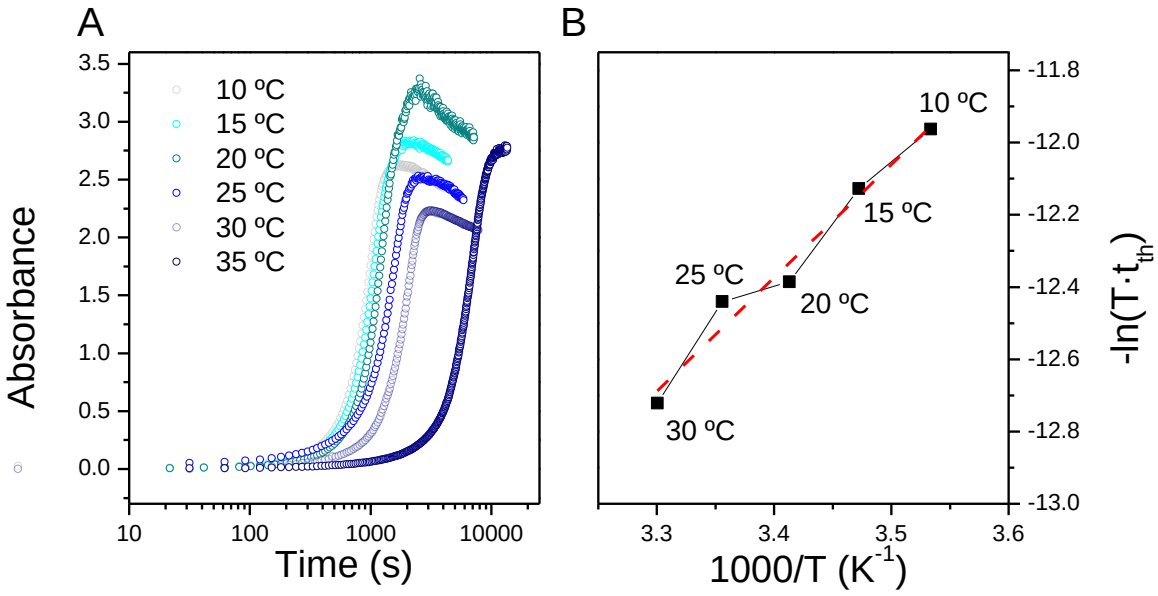

Figure 6. (A) Kinetic profiles obtained from turbidimetry as a function of temperature for the reaction of 5% γ-CD with 1% T90R4. (B) Plot of Eq. 2 used to determine the thermodynamic parameters of the reaction.

The complexation of γ-CD with the direct Tetronic, T904 gives rise to a more complex scenario: 1) PPO constitutes the central part of the macromolecule, thus is less accessible; 2) T904 self-assembles into micelles, with a critical micellar temperature (CMT) of 35 ºC for 1% T904.[48] For this reason, a separate data treatment below and above the CMT is necessary. Focusing first on the unimer region, up to 30 ºC, the kinetic curves are qualitatively similar to the ones obtained with T90R4 (SI, Figure 3A). The application of Eq. 2, using the calculated values of the number of CDs per arm of Tetronic (Figure 3D), yields negative $\Delta H^{\neq}$ and positive $\Delta S^{\neq}$ for the threading, as in T90R4 (Table 1). The overall Gibbs energy is negative (spontaneous process) but lower than for the reverse poloxamine (Table 1) and with no temperature dependence. The threading is clearly slower (Figure 5), due to the fact that the γ-CD has to thread on the PEO blocks first before reaching the inner four PPO blocks. If we assume that the γ-CD is located mainly on the PPO blocks (18 PO per arm), with two PO units included in a single γ-CD, the coverage of each block is not complete (only 10 POs groups are covered) under the conditions of the reaction (1% poloxamine and 5% of CD), as found also with T90R4.

Above the CMT, the threading time decreases substantially (Figure 5). The kinetic model rests upon the assumption of a single process taking place and it cannot be applied in this region, in which micelles coexist with unimers.

PPR formation of α-CD with T90R4 and T904

With the reverse Tetronic, under the same conditions used with γ-CD (5% CD + 1% T90R4), no PPR formation was detected with α-CD, in agreement with Harada et al.,[33] who first reported that α-CD does not complex with PO groups. However, working at a higher concentration (10% α-CD) produces a precipitate and the PPRs is formed with ca. 10 CDs per arm of Tetronic (Figure 3C). The kinetic profiles as a function of temperature are shown

in SI, Figure 4. Threading times are close to 10 min, with little effect of the temperature (SI, Figure 5), and in all cases, a break of the slope in the turbidity curves is observed above t_{th}. Overall, the curves diverge from the classic profile, probably reflecting a more complex threading process. It is clear, however, that by increasing the ratio of α-CD to polymer the reaction is forced to occur. The threading of α-CD through PPO blocks has been reported previously for Pluronics, where it is suggested that this CD only forms the PPR with the PEO blocks, while the PPO remains uncovered.[58] In our case, NMR studies show that there are 10 CDs threaded per arm of Tetronic (Figure 3C), meaning that α-CD is able to slide through both blocks to form the solid PPR.

With the direct poloxamine, T904, the kinetic curves show the classic profile (SI, Figure 3B), but the trend of the threading time differs from γ-CD (Figure 5), decreasing above 25ºC. Previous experiments have shown that the aggregation of Tetronics with temperature takes place in a gradual manner, [48] therefore, the presence of micelles at 25 and 30ºC (just below the CMT), cannot be discarded. We therefore focus here on the region up to 20ºC, far from the CMT, in which we can safely assume that the poloxamine is completely in the form of unimers.[48] Using the data treatment (Eq. 2), $\Delta H^{\neq}$ and $\Delta S^{\neq}$ are obtained (Table 1), which confirm the exothermic and entropy-driven character of the PPR formation. In this case, $\Delta H^{\neq}$ values are significantly higher than those obtained with the wider macrocycle, in line with the higher affinity of the EO for the α-CD, compared to γ-CD and PO. For comparison purposes, the kinetics of α-CD with a linear polyethylene glycol (PEG1000), at a concentration equivalent to that of the PEO blocks in T904, has been studied (SI, Figure 6). The reaction is significantly faster than with T904 (Figure 5), due to the lack of steric effects and the higher diffusivity of the polymer due to its smaller size. Data analysis with the Eyring equation shows that temperature hinders PPR formation (Table 1), as expected, and in

agreement with literature data[60,64–66], but overall the process is more spontaneous than for the reaction between α-CD and T904.

3.5. Time-resolved SANS experiments (TR-SANS)

The results described above provide information on the kinetics of aggregation of the PPRs over relatively long times, after t_{th}, rather than on the early stages corresponding to CDs threading onto the polymeric chains, since these do not give rise to turbidity. This stage can be studied conveniently by TR-SANS as the evolving neutron scattering patterns reflect variations in shape and/or size of the structures.

We focus first on the mixtures of γ-CD with T904 at 25ºC. Figure 7A shows the evolution of the scattering spectra over time. The overall intensity is very low, as it corresponds to the polymer in its unimer form, and the curves are quite noisy, due to the short exposure times used to capture changes at the beginning of the complexation. In previous investigations, a 4-arm star polymer model (4SP, see SI) has been successfully used to fit the scattering data from poloxamines pre-micellisation.[48,67,68] The same model was applied here, assuming that the shape of the PPR would not depart from this star structure upon threading of the macrocycle. With this assumption, the quadratic radius of gyration, R_g^2, was extracted by fitting the data at each timeframe, shown as a function of time in Figure 7B. Despite the large errors at short times, a weak steady, linear increase in size over time can be observed, which is consistent with the expansion of the PPR as the CDs thread along the polymer arms.

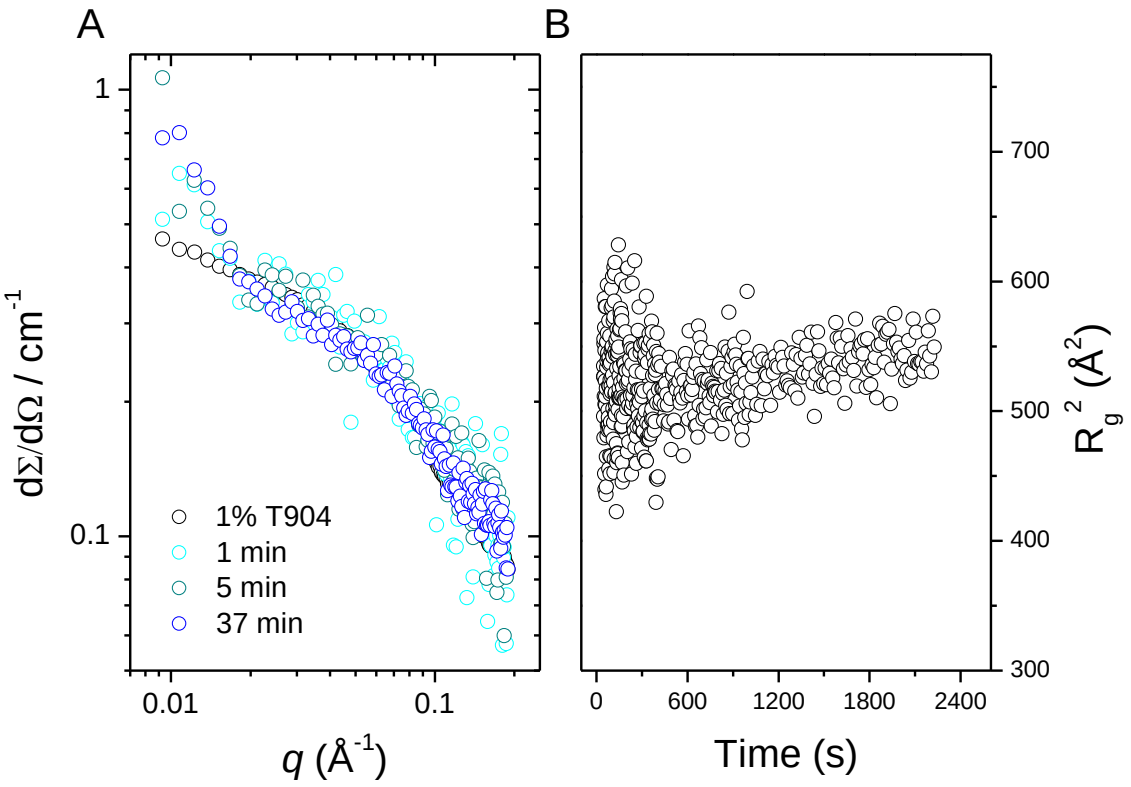

Figure 7. A) Time-resolved SANS spectra showing the formation of PPR with 3% γ-CD, and 1% T904 (25 ºC, in D_2O). B) quadratic radius of gyration, R_g^2, of the PPR, as obtained by fitting to a 4-arm star polymer model.

The description of the threading process of the CDs onto the polymer becomes more complex if the surfactant self-assembles into micelles, which is the case for T904 above the CMT, but with the benefit of a higher scattering and the consequent improvement of the signal-to-noise ratio. In this scenario, a competition is established between the threading of the macrocycle along the arms of the poloxamine and its self-aggregation.[37,48,53] We have considered the reaction of 1% T904 at 40 ºC, conditions in which the surfactant is aggregated and the scattering dominated by the micelles,[48] with 2.5% α-CD, which is below the threshold of formation of the insoluble PPR network (Figure 3), in order to avoid the scattering from large aggregates. Figure 8A shows the evolution of the scattering over time, in which the diminution of the intensity unambiguously shows the break-up of the micelles by the action of the CD. In principle, it would be possible to analyze the data by considering

the scattering from both the micelles and the evolving PPR (as a four-arm star polymer). Such a combined model has been successfully applied in the study of complexes of CDs with smaller surfactants, such as TPGS or metallosurfactants.[53,69] However, when comparing the scattering intensities shown in Figures 7A and 8A, it seems clear that the contribution of the free monomers is low, at a level similar to the background, which limits the application of this model. Hence, we have used a simplified approach which considers that there are mainly micelles in solution (core-shell spheres, CSS, see SI for details), thus neglecting the scattering from the unimers. The resulting fitted parameters are plotted in Figure 8. We observe that the presence of the macrocycle does not affect significantly either the radius or the thickness of the micelles (Figure 8B), nor the sld of the shell (Figure 8C), while their volume fraction diminishes monotonically as the reaction proceeds (Figure 8D). From this evidence, we can hypothesize that neither the α-CD nor the forming PPR take part in the T904 micelles can be drawn. Hence, upon mixing both components, the CDs thread the free poloxamine unimers to form the PPR, thus shifting the micellization equilibrium, which leads to the drop in micellar fraction observed.

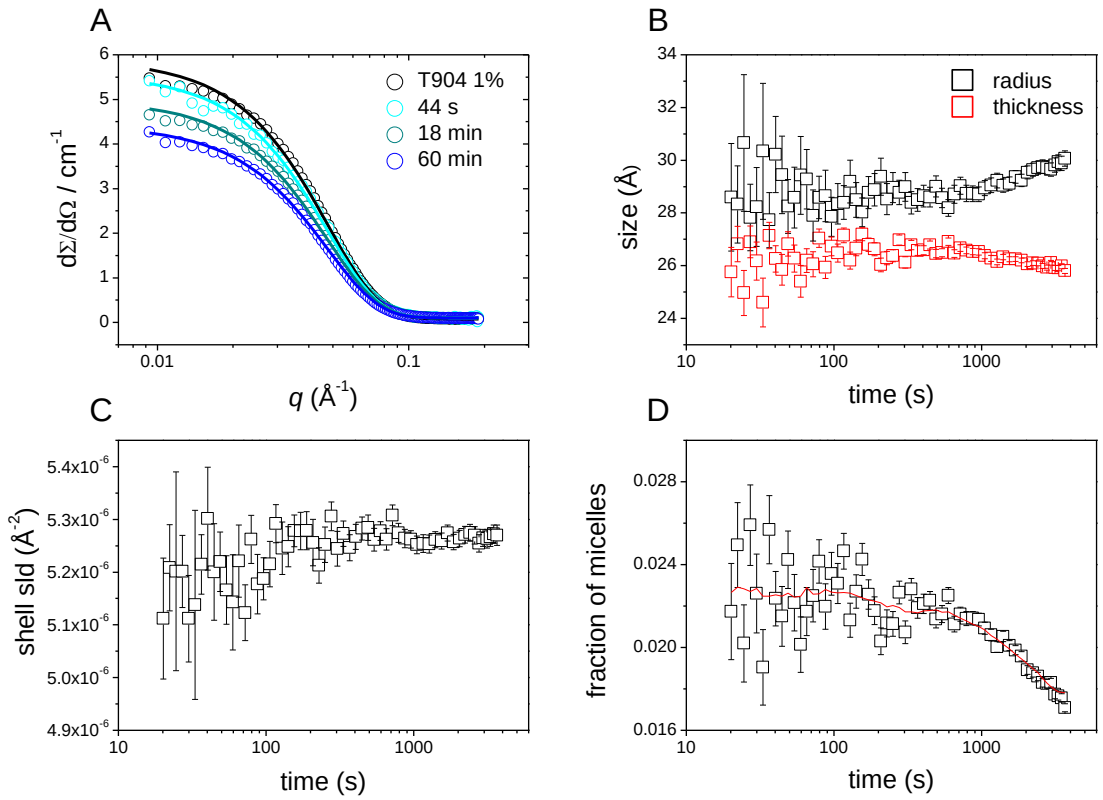

Figure 8. Time-resolved SANS kinetics showing the formation of PPR with 2.5% α-CD and 1% T904 (40 ºC, in D_2O). A) SANS spectra at selected time frames (y axis is in linear scale for better visualization). Solid lines correspond to fits to the core-shell sphere model; (B) evolution of the micellar size (core and thickness); (C) calculated scattering length density of the shell; (D) volume fraction of micelles.

The effect of CD on the break-up of the micelles is more noticeable when a higher amount of CD is used. Figure 9A shows the SANS spectra for selected frames of the kinetics run with 4% α-CD/1% T904. The overall shape of the curve is fairly constant up to 6 min, which mark the onset of the formation of larger structures associated with the packing of the PPRs, and detected as an upward trend at low *q*. This is in accordance with turbidimetry experiments performed in D_2O (SI, Figure 7). The analysis of the data must include in this case the contribution due to the scattering from the network, which can be modeled by a power law function (Porod exponent). It can be assumed that the micellar structural features are the same as those calculated for 1% T904, while the parameters that describe the

scattering of the PPRs aggregates are the Porod exponent and the scale factor (CSS-PL model, see details in SI). The resulting fitted parameters calculated with this approach are shown in Figure 9B. The effect of the network formation appears as a sharp turnout in the scale at exactly 6 min, while the volume fraction of the micelles follows the opposite trend, yet smoother. At short times, the curve shows a slight diminution of the volume fraction of the micelles, which corresponds to a shift of the micellization equilibrium, as observed at a lower α-CD concentration (Figure 8). Then, the volume fraction of the micelles drops quickly once the threading time (6 min) is reached. The aggregation of PPRs into large aggregates further shifts the equilibrium, quickly reducing the amount of unimers in solution, with the consequent reduction in micellar fraction.

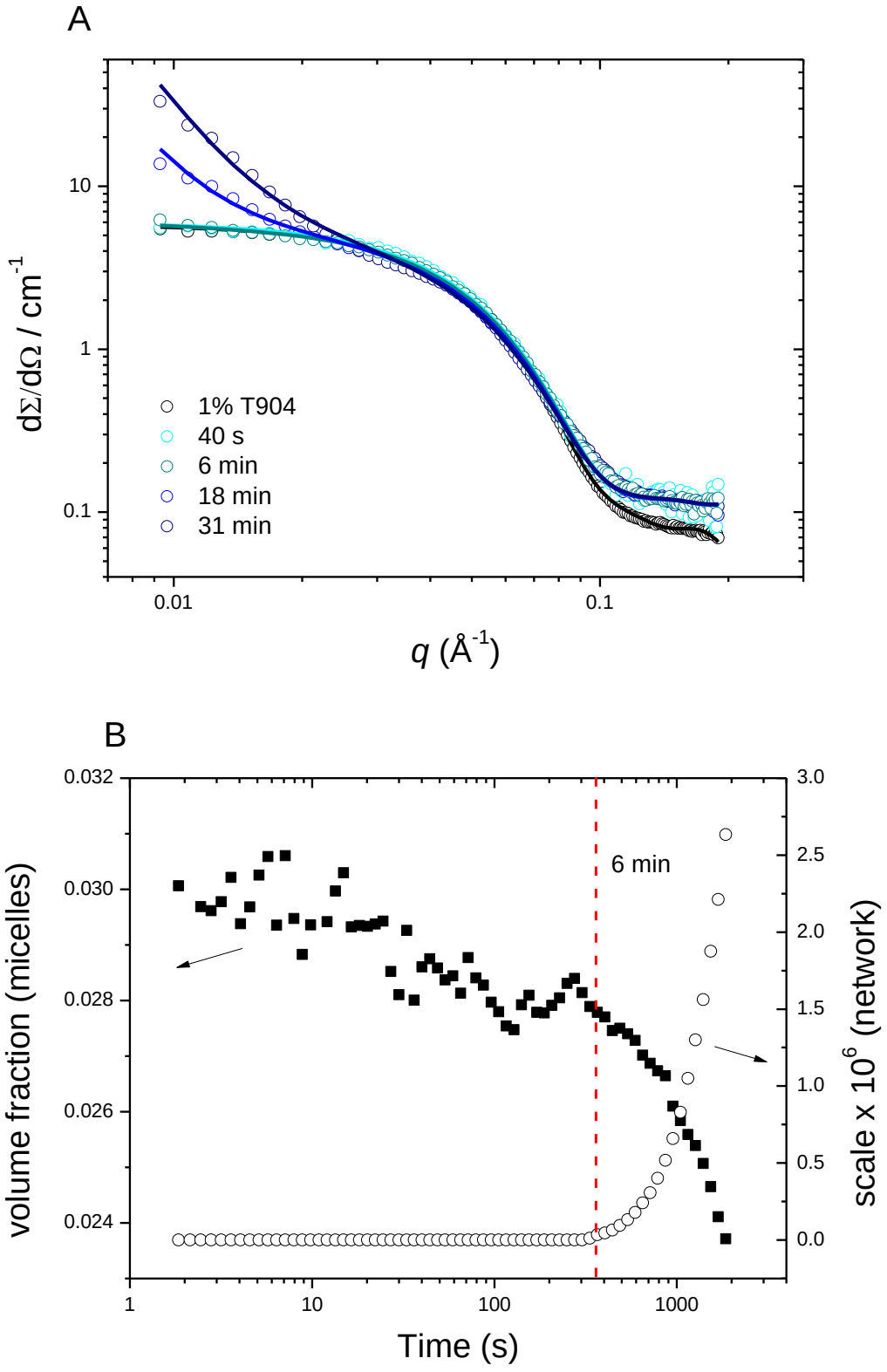

Figure 9. A) Time-resolved SANS kinetics showing the formation of PPR with 4% α-CD and 1% T904 (40 ºC, in D_2O). Solid lines correspond to fits to a CSS-PL model; B) Micellar volume fraction and scale of the PPR network. The red line marks the onset of the PPR self-aggregation (threading time).

4. Conclusions

PPR formation between native α- and γ-cyclodextrins (CDs) with tetrablock, X-shaped copolymers Tetronic 904 (T904) and Tetronic 90R4 (T90R4) has been investigated. Specifically, the impact that the inverted block position of the polymeric surfactants and cavity size of the CD have on the yield of the reaction, the final composition of the PPR, and thermodynamics and kinetics of the complexation were elucidated.

In the first stage, threading of the CDs on the arms of the poloxamines takes place. Interactions between CDs threaded on adjacent chains leads to the bundling and precipitation of the PPRs out of the solution, above a threshold concentration of the macrocycle, which varies with the type of CD and surfactant. With α-CD, a threshold concentration of 4 and 8% by weight is required to form the solid PPRs with 1% of T904 and T90R4, respectively. The precipitate contains crystalline channel-like structures that further organize into lamellar microstructures, as detected by SEM. In contrast, γ-CD produces the solid PPR over a wider concentration range, with increasing yields and number of CDs per arm threaded as the concentration increases. The results can be explained in terms of the preferential complexation of α-CD with EO monomers and γ-CD with PO units. With T904, the terminal PEO blocks are easily accessible to α-CD, whereas complexation with T90R4 involves threading over the PPO blocks, resulting in lower yields and increasing the threshold of α-CD required to achieve complexation. With the larger cavity γ-CD, threading over the PEO blocks in T904 to reach the middle PPO region is possible. The number of threaded CDs increases with the concentration of macrocycle, and at the highest concentration studied (12%) the number of macrocycles per arm is nearly the same for both CDs, around 10, which corresponds to a saturation of the poloxamines arms.

The different affinity of the CD for the two blocks has a direct impact on the kinetics of PPR formation (monitored by turbidimetry), due to the different presentation of these blocks on the two polymers. The kinetics of α-CD with T904 are much faster than with γ-CD, and no reaction (or a very slow one) is detected with T90R4, under the same conditions. In contrast, with the larger γ-CD, a similar kinetics profile, yet slower than with α-CD, is observed for both Tetronics.

Kinetic experiments were carried out at different temperatures to obtain the thermodynamic parameters of the complexation, using the theoretical framework based on the Eyring theory, the threading times, and the number of threaded CDs obtained from turbidimetry and NMR. Below the CMT of T904 (35ºC) and LCST of T90R4 (37ºC) the surfactant is in its unimer form and the reaction is spontaneous in all cases, with negative enthalpies and positive entropies, most favored in the case of α-CD with T904 and γ-CD with T90R4, in line with the corresponding affinity of these CDs for PEO and PPO blocks, respectively.

In the case of T904, above the micellization temperature, an equilibrium exists between micellisation and the formation of the PPR which, however, precludes the application of the Eyring model. Instead, the kinetics can be monitored conveniently by time-resolved small angle neutron scattering (TR-SANS), which give new insights into the reaction mechanism. In the case of the surfactants in the unimer form, TR-SANS reveal a slight increase in the radius of gyration of the polymer over time, consistent with the incorporation of the CDs onto the poloxamine arms and the subsequent expansion of the PPR. Above the CMT, the mixing of the micellized poloxamine and α-CD below the threshold concentration to form the precipitate leads to a reduction in the scattering intensity, which unambiguously shows the break-up of the micelles upon complexation with the macrocycle. Interestingly, the size and structure of the micelles do not change over time, but the micellar volume fraction

decreases. This suggests that neither the α-CD nor the PPR take part in T904 micelles and, that upon mixing both components, the CDs thread the free poloxamine to form PPRs, thus shifting the micellization equilibrium. This is also valid above the threshold concentration, where the reaction accelerates, and the aggregation of PPRs (leading to the onset of turbidity) shifts the micellar equilibrium, leading to a fast drop in the amount of unimers in solution, with a consequent reduction in the micellar fraction.

Acknowledgements

Authors acknowledge MINECO (Spain) for financial support through project MAT2014-59116-C2-2-R, and the Institut Laue-Langevin (ILL) for the provision of neutron beam time. J.P.-R. and R.S.-G. are grateful to the Asociación de Amigos de la Universidad de Navarra for their doctoral grant.

Supporting information

The supporting information is available free of charge on the ACS Publications website.

X-ray diffractogram of α-CD. Molar percentages of Tetronic and CD in the solid PPR as a function of the CD concentration. NMR analysis of the PPR at different reaction times. Kinetic profiles and threading times as a function of temperature for the reaction of α- and γ-CD with T904 and T90R4. Kinetic profiles for α-CD and PEG1000 as a function of temperature. Kinetic profiles of α-CD with T904 in D2O. Models used for TR-SANS data analysis with Sasview 4.2.0.

References

(1) Harada, A.; Li, J.; Kamachi, M. The Molecular Necklace: A Rotaxane Containing Many Threaded α-Cyclodextrins. *Nature* **1992**, *356* (6367), 325–327.

(2) Wenz, G. Cyclodextrins as Building Blocks for Supramolecular Structures and

Functional Units. *Angew. Chemie Int. Ed. English* **1994**, *33* (8), 803–822.

(3) Nepogodiev, S. A.; Stoddart, J. F. Cyclodextrin-Based Catenanes and Rotaxanes. *Chem. Rev.* **1998**, *98* (5), 1959–1976.

(4) Ashton, P. R.; Grognuz, M.; Slawin, A. M. Z.; Stoddart, J. F.; Williams, D. J. The Template-Directed Synthesis of a [2]rotaxane. *Tetrahedron Lett.* **1991**, *32* (43), 6235–6238.

(5) Nobel Media AB. Sir J. Fraser Stoddart - Facts http://www.nobelprize.org/nobel_prizes/chemistry/laureates/2016/stoddart-facts.html (accessed Jun 5, 2018).

(6) Perry, C.; Hébraud, P.; Gernigon, V.; Brochon, C.; Lapp, A.; Lindner, P.; Schlatter, G. Pluronic and β-Cyclodextrin in Water: From Swollen Micelles to Self-Assembled Crystalline Platelets. *Soft Matter* **2011**, *7* (7), 3502–3512.

(7) Simoes, S. M. N.; Rey-Rico, A.; Concheiro, A.; Alvarez-Lorenzo, C. Supramolecular Cyclodextrin-Based Drug Nanocarriers. *Chem. Commun.* **2015**, *51* (29), 6275–6289.

(8) Li, J.; Loh, X. Cyclodextrin-Based Supramolecular Architectures: Syntheses, Structures, and Applications for Drug and Gene Delivery. *Adv. Drug Deliv. Rev.* **2008**, *60* (9), 1000–1017.

(9) Zhang, J.; Ma, P. X. Cyclodextrin-Based Supramolecular Systems for Drug Delivery: Recent Progress and Future Perspective. *Adv. Drug Deliv. Rev.* **2013**, *65* (9), 1215–1233.

(10) Garcia-Rio, L.; Otero-Espinar, F. J.; Luzardo-Alvarez, A.; Blanco-Mendez, J. Cyclodextrin Based Rotaxanes, Polyrotaxanes and Polypseudorotaxanes and Their Biomedical Applications. *Curr. Top. Med. Chem.* **2014**, *14* (4), 478–493.

(11) Choi, S.; Kwon, T. W.; Coskun, A.; Choi, J. W. Highly Elastic Binders Integrating Polyrotaxanes for Silicon Microparticle Anodes in Lithium Ion Batteries. *Science.*

2017, *357* (6348), 279–283.

(12) Imholt, L.; Dong, D.; Bedrov, D.; Cekic-Laskovic, I.; Winter, M.; Brunklaus, G. Supramolecular Self-Assembly of Methylated Rotaxanes for Solid Polymer Electrolyte Application. *ACS Macro Lett.* **2018**, *7* (7), 881–885.

(13) Jiang, L.; Kato, K.; Mayumi, K.; Yokoyama, H.; Ito, K. One-Pot Synthesis and Characterization of Polyrotaxane–Silica Hybrid Aerogel. *ACS Macro Lett.* **2017**, *6* (3), 281–286.

(14) Wang, J.; Du, R.; Zhang, X. Thermoresponsive Polyrotaxane Aerogels: Converting Molecular Necklaces into Tough Porous Monoliths. *ACS Appl. Mater. Interfaces* **2018**, *10* (2), 1468–1473.

(15) Szejtli, J. Introduction and General Overview of Cyclodextrin Chemistry. *Chem. Rev.* **1998**, *98* (5), 1743–1754.

(16) Davis, M. E.; Brewster, M. E. Cyclodextrin-Based Pharmaceutics: Past, Present and Future. *Nat. Rev. Drug Discov.* **2004**, *3* (12), 1023–1035.

(17) Harada, A. Preparation and Structures of Supramolecules between Cyclodextrins and Polymers. *Coord. Chem. Rev.* **1996**, *148*, 115–133.

(18) Pozuelo, J.; Mendicuti, F.; Mattice, W. L. Inclusion Complexes of Chain Molecules with Cycloamyloses. 2. Molecular Dynamics Simulations of Polyrotaxanes Formed by Poly(ethylene Glycol) and α-Cyclodextrins. *Macromolecules* **1997**, *30* (12), 3685–3690.

(19) Kong, T.; Ye, L.; Zhang, A.; Feng, Z. How Does PHEMA Pass through the Cavity of γ-CDs to Create Mismatched Overfit Polypseudorotaxanes? *Langmuir* **2018**, *34* (46), 14076–14084.

(20) Wenz, G.; Han, B. H.; Müller, A. Cyclodextrin Rotaxanes and Polyrotaxanes. *Chem. Rev.* **2006**, *106* (3), 782–817.

(21) González-Gaitano, G.; Isasi, J. R.; Vélaz, I.; Zornoza, A. Drug Carrier Systems Based On Cyclodextrin Supramolecular Assemblies And Polymers: Present And Perspectives. *Curr. Pharm. Des.* **2017**, *23* (3).

(22) Yu, G.; Yang, Z.; Fu, X.; Yung, B. C.; Yang, J.; Mao, Z.; Shao, L.; Hua, B.; Liu, Y.; Zhang, F.; et al. Polyrotaxane-Based Supramolecular Theranostics. *Nat. Commun.* **2018**, *9* (1), 1–13.

(23) Liu, K. L.; Zhang, Z.; Li, J. Supramolecular Hydrogels Based on Cyclodextrin–polymer Polypseudorotaxanes: Materials Design and Hydrogel Properties. *Soft Matter* **2011**, *7* (24), 11290–11297.

(24) Harada, A.; Kamachi, M. Complex Formation between Poly(ethylene Glycol) and α-Cyclodextrin. *Macromolecules* **1990**, *23* (10), 2821–2823.

(25) Harada, A.; Li, J.; Kamachi, M. Synthesis of a Tubular Polymer from Threaded Cyclodextrins. *Nature* **1993**, *364* (6437), 516–518.

(26) Tsai, C. C.; Leng, S.; Jeong, K. U.; Van Horn, R. M.; Wang, C. L.; Zhang, W. B.; Graham, M. J.; Huang, J.; Ho, R. M.; Chen, Y.; et al. Supramolecular Structure of β-Cyclodextrin and Poly(ethylene Oxide)-Block-Poly(propylene Oxide)-Block-Poly(ethylene Oxide) Inclusion Complexes. *Macromolecules* **2010**, *43* (22), 9454–9461.

(27) Alexandridis, P.; Athanassiou, V.; Fukuda, S.; Hatton, T. A. Surface Activity of Poly(ethylene Oxide)-Block-Poly(propylene Oxide)-Block-Poly(ethylene Oxide) Copolymers. *Langmuir* **1994**, *10* (8), 2604–2612.

(28) Alexandridis, P.; Holzwarth, J. F.; Hatton, T. A. Micellization of Poly(ethylene Oxide)-Poly(propylene Oxide)-Poly(ethylene Oxide) Triblock Copolymers in Aqueous Solutions: Thermodynamics of Copolymer Association. *Macromolecules* **1994**, *27* (9), 2414–2425.

(29) Nagarajan, R. Solubilization of Hydrocarbons and Resulting Aggregate Shape Transitions in Aqueous Solutions of Pluronic® (PEO–PPO–PEO) Block Copolymers. *Colloids Surfaces B Biointerfaces* **1999**, *16* (1–4), 55–72.

(30) Kabanov, A. V.; Batrakova, E. V; Alakhov, V. Y. Pluronic® Block Copolymers as Novel Polymer Therapeutics for Drug and Gene Delivery. *J. Control. Release* **2002**, *82* (2–3), 189–212.

(31) Larrañeta, E.; Isasi, J. R. Phase Behavior of Reverse Poloxamers and Poloxamines in Water. *Langmuir* **2013**, *29* (4), 1045–1053.

(32) Harada, A.; Li, J.; Kamachi, M. Preparation and Properties of Inclusion Complexes of Polyethylene Glycol with Alpha-Cyclodextrin. *Macromolecules* **1993**, *26* (21), 5698–5703.

(33) Harada, A.; Okada, M.; Li, J.; Kamachi, M. Preparation and Characterization of Inclusion Complexes of Poly(propylene Glycol) with Cyclodextrins. *Macromolecules* **1995**, *28* (24), 8406–8411.

(34) Gaitano, G. G.; Brown, W.; Tardajos, G. Inclusion Complexes between Cyclodextrins and Triblock Copolymers in Aqueous Solution: A Dynamic and Static Light-Scattering Study. *J. Phys. Chem. B* **1997**, *101* (5), 710–719.

(35) Dreiss, C. A.; Nwabunwanne, E.; Liu, R.; Brooks, N. J. Assembling and de-Assembling Micelles: Competitive Interactions of Cyclodextrins and Drugs with Pluronics. *Soft Matter* **2009**, *5* (9), 1888–1896.

(36) Bleta, R.; Machut, C.; Léger, B.; Monflier, É.; Ponchel, A. Coassembly of Block Copolymer and Randomly Methylated β-Cyclodextrin: From Swollen Micelles to Mesoporous Alumina with Tunable Pore Size. *Macromolecules* **2013**, *46* (14), 5672–5683.

(37) Valero, M.; Grillo, I.; Dreiss, C. A. Rupture of Pluronic Micelles by Di-Methylated

β-Cyclodextrin Is Not Due to Polypseudorotaxane Formation. *J. Phys. Chem. B* **2012**, *116* (4), 1273–1281.

(38) Castiglione, F.; Valero, M.; Dreiss, C. A.; Mele, A. Selective Interaction of 2,6-Di-O-Methyl-β-Cyclodextrin and Pluronic F127 Micelles Leading to Micellar Rupture: A Nuclear Magnetic Resonance Study. *J. Phys. Chem. B* **2011**, *115* (29), 9005–9013.

(39) Nogueiras-Nieto, L.; Alvarez-Lorenzo, C.; Sandez-Macho, I.; Concheiro, A.; Otero-Espinar, F. J. Hydrosoluble Cyclodextrin/Poloxamer Polypseudorotaxanes at the Air/Water Interface, in Bulk Solution, and in the Gel State. *J. Phys. Chem. B* **2009**, *113* (9), 2773–2782.

(40) Mondjinou, Y. A.; McCauliff, L. A.; Kulkarni, A.; Paul, L.; Hyun, S.-H.; Zhang, Z.; Wu, Z.; Wirth, M.; Storch, J.; Thompson, D. H. Synthesis of 2-Hydroxypropyl-β-cyclodextrin/Pluronic-Based Polyrotaxanes via Heterogeneous Reaction as Potential Niemann-Pick Type C Therapeutics. *Biomacromolecules* **2013**, *14* (12), 4189–4197.

(41) Collins, C. J.; Loren, B. P.; Alam, M. S.; Mondjinou, Y.; Skulsky, J. L.; Chaplain, C. R.; Haldar, K.; Thompson, D. H. Pluronic Based β-Cyclodextrin Polyrotaxanes for Treatment of Niemann-Pick Type C Disease. *Sci. Rep.* **2017**, *7*, 1–13.

(42) Tamura, A.; Ohashi, M.; Yui, N. Oligo(ethylene Glycol)-Modified β-Cyclodextrin-Based Polyrotaxanes for Simultaneously Modulating Solubility and Cellular Internalization Efficiency. *J. Biomater. Sci. Polym. Ed.* **2017**, *28* (10–12), 1124–1139.

(43) Cuestas, M. L.; Sosnik, A.; Mathet, V. L. Poloxamines Display a Multiple Inhibitory Activity of ATP-Binding Cassette (ABC) Transporters in Cancer Cell Lines. *Mol. Pharm.* **2011**, *8* (4), 1152–1164.

(44) Alvarez-Lorenzo, C.; Sosnik, A.; Concheiro, A. PEO-PPO Block Copolymers for Passive Micellar Targeting and Overcoming Multidrug Resistance in Cancer Therapy. *Curr. Drug Targets* **2011**, *12* (8), 1112–1130.

(45) Larrañeta, E.; Isasi, J. R. Self-Assembled Supramolecular Gels of Reverse Poloxamers and Cyclodextrins. *Langmuir* **2012**, *28* (34), 12457–12462.

(46) Larrañeta, E.; Martínez-Ohárriz, C.; Vélaz, I.; Zornoza, A.; Machín, R.; Isasi, J. R. In Vitro Release from Reverse Poloxamine/α-Cyclodextrin Matrices: Modelling and Comparison of Dissolution Profiles. *J. Pharm. Sci.* **2014**, *103* (1), 197–206.

(47) Larrañeta, E.; Isasi, J. R. Non-Covalent Hydrogels of Cyclodextrins and Poloxamines for the Controlled Release of Proteins. *Carbohydr. Polym.* **2014**, *102*, 674–681.

(48) González-Gaitano, G.; Müller, C.; Radulescu, A.; Dreiss, C. A. Modulating the Self-Assembly of Amphiphilic X-Shaped Block Copolymers with Cyclodextrins: Structure and Mechanisms. *Langmuir* **2015**, *31* (14), 4096–4105.

(49) Rey-Rico, A.; Babicz, H.; Madry, H.; Concheiro, A.; Alvarez-Lorenzo, C.; Cucchiarini, M. Supramolecular Polypseudorotaxane Gels for Controlled Delivery of rAAV Vectors in Human Mesenchymal Stem Cells for Regenerative Medicine. *Int. J. Pharm.* **2017**, *531* (2), 492–503.

(50) Shen, J.; Xu, G.; Xin, X.; Wang, L.; Song, Z.; Zhang, H.; Tong, L.; Yang, Z. Supramolecular Hydrogels of α-Cyclodextrin/reverse Poloxamines/carbon-Based Nanomaterials and Its Multi-Functional Application. *RSC Adv.* **2015**, *5* (50), 40173–40182.

(51) Dreiss, C. A.; González-Gaitano, G.; Grillo, I.; Serra-Gómez, R. Unravelling the Mechanisms of Complexation between Tetronics and Cyclodextrins. *Inst. Laue-Langevin* **2015**, http://doi.ill.fr/10.5291/ILL-DATA.9-12-401.

(52) M. Doucet, et al. SasView Version 4.2, http://doi.org/10.5281/zenodo.1412041.

(53) Puig-Rigall, J.; Grillo, I.; Dreiss, C. A.; González-Gaitano, G. Structural and Spectroscopic Characterization of TPGS Micelles: Disruptive Role of Cyclodextrins and Kinetic Pathways. *Langmuir* **2017**, *33* (19), 4737–4747.

(54) Rusa, C. C.; Rusa, M.; Peet, J.; Uyar, T.; Fox, J.; Hunt, M. A.; Wang, X.; Balik, C. M.; Tonelli, A. E. The Nano-Threading of Polymers. *J. Incl. Phenom. Macrocycl. Chem.* **2006**, *55* (1–2), 185–192.

(55) Hunt, M. A.; Tonelli, A. E.; Balik, C. M. Effect of Guest Hydrophobicity on Water Sorption Behavior of Oligomer/α-Cyclodextrin Inclusion Complexes. *J. Phys. Chem. B* **2007**, *111* (15), 3853–3858.

(56) Narayanan, G.; Aguda, R.; Hartman, M.; Chung, C. C.; Boy, R.; Gupta, B. S.; Tonelli, A. E. Fabrication and Characterization of Poly(ε-Caprolactone)/α-Cyclodextrin Pseudorotaxane Nanofibers. *Biomacromolecules* **2016**, *17* (1), 271–279.

(57) Oster, M.; Hébraud, A.; Gallet, S.; Lapp, A.; Pollet, E.; Avérous, L.; Schlatter, G. Star-Pseudopolyrotaxane Organized in Nanoplatelets for Poly(ε-Caprolactone)-Based Nanofibrous Scaffolds with Enhanced Surface Reactivity. *Macromol. Rapid Commun.* **2015**, *36* (3), 292–297.

(58) Li, J.; Ni, X. P.; Leong, K. Block-Selected Molecular Recognition and Formation of Polypseudorotaxanes between Poly(propylene Oxide)-Poly(ethylene Oxide)-Poly(propylene Oxide) Triblock Copolymers and α-Cyclodextrin. *Angew. Chemie Int. Ed.* **2003**, *42* (1), 69–72.

(59) Lo Nostro, P.; Lopes, J. R.; Cardelli, C. Formation of Cyclodextrin-Based Polypseudorotaxanes: Solvent Effect and Kinetic Study. *Langmuir* **2001**, *17* (15), 4610–4615.

(60) Lo Nostro, P.; Giustini, L.; Fratini, E.; Ninham, B. W.; Ridi, F.; Baglioni, P. Threading, Growth, and Aggregation of Pseudopolyrotaxanes. *J. Phys. Chem. B* **2008**, *112* (4), 1071–1081.

(61) Serres-Gómez, M.; González-Gaitano, G.; Kaldybekov, D. B.; Mansfield, E. D. H.; Khutoryanskiy, V. V.; Isasi, J. R.; Dreiss, C. A. Supramolecular Hybrid Structures

and Gels from Host–Guest Interactions between α-Cyclodextrin and PEGylated Organosilica Nanoparticles. *Langmuir* **2018**, *34* (36), 10591–10602.

(62) Ceccato, M.; Lo Nostro, P.; Baglioni, P. α-Cyclodextrin/Polyethylene Glycol Polyrotaxane: A Study of the Threading Process. *Langmuir* **1997**, *13* (9), 2436–2439.

(63) Becheri, A.; Lo Nostro, P.; Ninham, B. W.; Baglioni, P. The Curious World of Polypseudorotaxanes: Cyclodextrins as Probes of Water Structure. *J. Phys. Chem. B* **2003**, *107* (16), 3979–3987.

(64) Dreiss, C. A.; Cosgrove, T.; Newby, F. N.; Sabadini, E. Formation of a Supramolecular Gel between α-Cyclodextrin and Free and Adsorbed PEO on the Surface of Colloidal Silica: Effect of Temperature, Solvent, and Particle Size. *Langmuir* **2004**, *20* (21), 9124–9129.

(65) Peet, J.; Rusa, C. C.; Hunt, M. A.; Tonelli, A. E.; Balik, C. M. Solid-State Complexation of Poly(Ethylene Glycol) with α−Cyclodextrin. *Macromolecules* **2005**, *38* (2), 537–541.

(66) Travelet, C.; Schlatter, G.; Hébraud, P.; Brochon, C.; Lapp, A.; Hadziioannou, G. Formation and Self-Organization Kinetics of α-CD/PEO-Based Pseudo-Polyrotaxanes in Water. A Specific Behavior at 30 °C. *Langmuir* **2009**, *25* (15), 8723–8734.

(67) González-Gaitano, G.; da Silva, M. A.; Radulescu, A.; Dreiss, C. A. Selective Tuning of the Self-Assembly and Gelation of a Hydrophilic Poloxamine by Cyclodextrins. *Langmuir* **2015**, *31* (20), 5645–5655.

(68) Serra-Gómez, R.; Dreiss, C. A.; González-Benito, J.; González-Gaitano, G. Structure and Rheology of Poloxamine T1107 and Its Nanocomposite Hydrogels with Cyclodextrin-Modified Barium Titanate Nanoparticles. *Langmuir* **2016**, *32* (25), 6398–6408.

(69) Iza, N.; Guerrero-Martínez, A.; Tardajos, G.; Ortiz, M. J.; Palao, E.; Montoro, T.; Radulescu, A.; Dreiss, C. A.; González-Gaitano, G. Using Inclusion Complexes with Cyclodextrins To Explore the Aggregation Behavior of a Ruthenium Metallosurfactant. *Langmuir* **2015**, *31* (9), 2677–2688.

For Table of Contents use only

Pseudo-Polyrotaxanes of Cyclodextrins with Direct and Reverse X-shaped Block-Copolymers: a Kinetic and Structural Study

Joan Puig-Rigall[1], Rafael Serra-Gómez[1], Ian Stead[2], Isabelle Grillo[3], Cécile A. Dreiss*[,2] and Gustavo González-Gaitano*[,1]